Received: 6 December 2021 | Accepted: 1 May 2022

DOI: 10.1002/hep4.2011

ORIGINAL ARTICLE

Combinations of an acetyl CoA carboxylase inhibitor with hepatic lipid modulating agents do not augment antifibrotic efficacy in preclinical models of NASH and fibrosis

Archana Vijayakumar | Ayse Okesli-Armlovich | Ting Wang | Isabel Olson | Minji Seung | Saritha Kusam | David Hollenback | Sangeetha Mahadevan | Bruno Marchand | Maria Toteva | David G. Breckenridge | James L. Trevaskis | Jamie Bates

Gilead Sciences, Foster City, California, USA

Correspondence
Ayse Okesli-Armlovich, Gilead Sciences, 333 Lakeside Drive, Foster City, CA, USA.
Email: ayse.okesli-armlovich@gilead.com

Funding information
Gilead Sciences

Abstract

Dysregulated hepatocyte lipid metabolism is a hallmark of hepatic lipotoxicity and contributes to the pathogenesis of nonalcoholic steatohepatitis (NASH). Acetyl CoA carboxylase (ACC) inhibitors decrease hepatocyte lipotoxicity by inhibiting *de novo* lipogenesis and concomitantly increasing fatty acid oxidation (FAO), and firsocostat, a liver-targeted inhibitor of ACC1/2, is under evaluation clinically in patients with NASH. ACC inhibition is associated with improvements in indices of NASH and reduced liver triglyceride (TG) content, but also increased circulating TG in subjects with NASH and preclinical rodent models. Here we evaluated whether enhancing hepatocyte FAO by combining ACC inhibitors with peroxisomal proliferator-activated receptor (PPAR) or thyroid hormone receptor beta (THRβ) agonists could drive greater liver TG reduction and NASH/antifibrotic efficacy, while ameliorating ACC inhibitor–induced hypertriglyceridemia. In high-fat diet–fed dyslipidemic rats, the addition of PPAR agonists fenofibrate (Feno), elafibranor (Ela), lanifibranor (Lani), seladelpar (Sela) or saroglitazar (Saro), or the THRb agonist resmetirom (Res), to an analogue of firsocostat (ACCi) prevented ACCi-induced hypertriglyceridemia. However, only PPARα agonists (Feno and Ela) and Res provided additional liver TG reduction. In the choline-deficient high-fat diet rat model of advanced liver fibrosis, neither PPARα (Feno) nor THRβ (Res) agonism augmented the antifibrotic efficacy of ACCi. *Conclusion*: These data suggest that combination therapies targeting hepatocyte lipid metabolism may have beneficial effects on liver TG reduction; however, they may not be sufficient to drive fibrosis regression.

INTRODUCTION

Nonalcoholic steatohepatitis (NASH) is a progressive form of nonalcoholic fatty liver disease (NAFLD) that is characterized by liver injury, including hepatocyte ballooning, inflammation and progressive fibrosis, and is estimated to affect 2%–5% (or 16 million) of the adult US population.[1–4] Furthermore, NAFLD/NASH is the hepatic manifestation of metabolic syndrome, a constellation of conditions that increase risk for cardiovascular disease and type 2 diabetes. NASH represents a significant and growing unmet medical need and is expected to become the leading cause for liver transplants in the United States.[5,6]

A growing body of evidence suggests that accumulation of lipotoxic intermediates, such as nonesterified fatty acids (NEFAs), in the liver contributes to NASH pathogenesis.[7] This is attributed to dysregulated hepatic lipid metabolism, mediated by increased *de novo* lipogenesis (DNL) and/or aberrant fatty acid oxidation (FAO), and increased influx of extrahepatic NEFA from adipose tissue lipolysis and/or dietary triglycerides (TG) breakdown.[8] Several therapies under investigation for the treatment of NASH target hepatic lipid metabolism via several mechanisms, including reducing DNL (acetyl CoA carboxylase [ACC1] and fatty acid synthase inhibitors), increasing FAO (peroxisome proliferator–activated receptor [PPAR] and thyroid hormone receptor beta [THRβ] agonists, as well as ACC2 inhibition), and improving systemic insulin sensitivity to decrease extrahepatic NEFA production (glucagon-like peptide 1 receptor agonists).[9]

Firsocostat (FIR), a liver-directed allosteric ACC1/2 inhibitor, provides an attractive strategy to reduce hepatic lipid burden by simultaneously inhibiting DNL and increasing FAO.[10] FIR treatment significantly reduced liver lipid content and biomarkers of hepatocyte injury (alanine aminotransferase [ALT] and aspartate aminotransferase [AST]) and fibrosis (tissue inhibitor of metalloproteinase 1 [TIMP1]) in patients with NASH.[11,12] A liver-targeted analog of FIR (GS-834356; ACCi) mimics these effects in preclinical species, with dose-dependent reductions in hepatic steatosis and prevention of fibrosis progression in rodents, which in part may be driven by direct inhibition of hepatic stellate cell (HSC) activation.[13,14]

Clinical ACC inhibition causes an on-target elevation of circulating TG, especially in subjects with elevated baseline TG.[11,12] This observation is recapitulated preclinically with pharmacological inhibition or genetic deletion of ACC.[13,15,16] Preclinical transcriptomic and lipidomic analyses of livers of fast-food diet (FFD)–fed mice treated with ACCi revealed a signature for reduced PPARα activity.[13] Indeed, fenofibrate (Feno), a PPARα agonist, completely mitigates FIR or ACCi-induced hypertriglyceridemia in subjects with NASH and FFD mice, respectively.[13,17] Several PPAR agonists with greater potency than Feno and/or differential PPAR isoform selectivity are in various stages of clinical development for NASH, including elafibranor (Ela; PPARα/δ), lanifibarnor (Lani; pan-PPAR), seladelpar (Sela; PPARδ), and saroglitazar (Saro; PPARα/γ).[18] Here, we profiled whether combinations of ACCi with PPAR agonists in clinical development for NASH (including Ela, Lani, Sela, and Saro) could mitigate ACCi-induced increase in circulating TG, while achieving comparable or better liver TG reduction than ACCi/Feno combination in a dyslipidemic rat model. Furthermore, we sought to evaluate the NASH and antifibrotic efficacy of combinations that ameliorated ACCi-induced circulating TG increase.

THRβ agonism represents an orthogonal mechanism to PPAR agonism to increase hepatic FAO and Resmetirom (Res), a liver-targeted THRβ agonist, has been shown to improve plasma lipid profiles and promote hepatic TG reduction and NASH resolution clinically.[19] Therefore, we also compared the effect of ACCi/Res combinations on circulating and liver TG, and NASH and fibrosis efficacy in our preclinical models.

Of all the agents tested, only PPARα agonism with Feno or Ela, and THRβ agonism with Res, demonstrated additional liver TG reduction than ACCi monotherapy, while all agents dose-dependently mitigated ACCi-induced circulating TG increase. Furthermore, neither Feno nor Res enhanced the antifibrotic efficacy of ACCi, suggesting that combinations targeting hepatocyte lipotoxicity may not be sufficient to enhance NASH or antifibrotic efficacy.

METHODS

Animal studies

All animal procedures were in compliance with the U.S. Department of Agriculture's Animal Welfare Act (9 CFR Parts 1, 2, and 3), the Guide for the Care and Use of Laboratory Animals (Institute for Laboratory Animal Research, The National Academies Press, Washington DC), and the National Institutes of Health, Office of Laboratory Animal Welfare. A total of five *in vivo* studies were performed in three models as outlined in Table S1. For the FFD mouse and dyslipidemic rat models, animals were fed FFD (D12079B; Research Diets) with 4.03% sugar water (2.3% [wt/vol] fructose +1.7% [wt/vol] glucose) for 54 and 4 weeks, respectively, and treated with test article as outlined in Table S1. In the dyslipidemic rat studies, animals were predosed with PPAR or THRβ agonist for 1 week before initiation of ACCi treatment. Doses of PPAR/THRβ agonists were determined from previous publications.[20–24] The choline-deficient high-fat diet (CDHFD) rat model of fibrosis has been described previously.[14] Briefly, animals were placed on the CDHFD (A16092003;

Research Diets), L-amino acid diet with 45 kcal% fat with 0.1% methionine, no added choline and 1% cholesterol) for a total of 12 weeks and treated with test article from weeks 6–12 as outlined in Table S1. Primary endpoints measured included circulating and liver TG, β-hydroxybutyrate (BHB) and acylcarnitines, and immunostaining liver sections for immune cell and fibrogenesis markers (FFD mouse model), circulating and liver TG (rat dyslipidemic model), liver picrosirius red (PSR) staining, immunostaining liver sections for immune cell and fibrogenesis markers, and plasma levels of biomarkers of liver health and function (CDHFD rat model), as described previously[14] and in the Supporting Methods.

FAO assay

Huh7 cells were cultured in Dulbecco's modified Eagle medium supplemented with 10% fetal bovine serum and 1% penicillin–streptomycin. Briefly, cells were seeded at 1×10^5 cells/well, starved for 1 h in FAO assay media, treated with compounds (1% final DMSO concentration) and ^{14}C-oleic acid (0.1 uCi/ul), and incubated overnight. Acid soluble material was extracted from the supernatant using 60% perchloric acid and quantified by scintillation counting.

Statistical analysis

Unless otherwise specified, all data are presented as mean ± SEM. For *in vivo* studies, statistical analyses were performed using nonparametric Mann–Whitney test to compare two groups or Kruskal-Wallis with Dunn's correction for comparison of three or more groups (p-value ≤ 0.05 was considered statistically significant).

RESULTS

ACCi/Feno combination had beneficial synergistic effects in the FFD mouse model of early NASH

Relative to ACCi monotherapy, ACCi/Feno combination caused further liver TG reduction and normalized circulating TG in the FFD mouse model of early NASH.[13] In this study, we expanded the analysis to assess mechanisms contributing to the synergistic effects of ACCi/Feno combination on liver TG and potential effects on NASH endpoints. Mice were fed FFD for 8 months and dosed with ACCi, Feno^{low} (50 mg/kg) and Feno^{high} (150 mg/kg), alone or in combination with ACCi, for 14 days. Terminal plasma and liver concentrations of Feno changed dose-dependently, and exposures of Feno and ACCi were not altered between monotherapy and combination arms (Figure S1A).

Feno^{high} caused significant weight loss (8%–11%) in the monotherapy and combination groups (Figure 1A). ACCi, but not Feno, monotherapy significantly decreased liver TG by 22%, and ACCi/Feno combinations further reduced liver TG (40%–45% vs. vehicle; $p \leq 0.01$ vs. ACCi) (Figure 1B). Liver total cholesterol content was significantly reduced by 49%, 57%, and 18% with Feno^{low}, Feno^{high}, and ACCi monotherapy, respectively, and greater reductions (58%–66%) were observed with ACCi/Feno combinations (Figure S1B). Compared with vehicle, plasma and hepatic β-hydroxy butyrate (BHB) levels increased dose-dependently with Feno (2-4×) and ACCi (2×) monotherapy. ACCi/Feno combinations synergistically increased plasma (4-7×) and liver (4–5×) BHB levels relative to ACCi or Feno alone (Figure 1C,D). In plasma, ACCi monotherapy reduced several species of short and medium-chain acylcarnitines, while ACCi/Feno combination reduced and even normalized several short, medium, and long-chain acylcarnitine species (Figure 1E). In the liver, Feno monotherapy tended to increase long-chain acylcarnitine species while ACCi monotherapy decreased them. The hepatic acylcarnitine profile with ACCi/Feno combination was similar to Feno monotherapy (Figure 1F). These data indicate that ACCi/Feno synergistically increased lipid oxidation in the liver, resulting in additional liver TG reduction.

Plasma FGF21 levels were significantly decreased by 41% with ACCi monotherapy, and dose-dependently and similarly increased with Feno monotherapy and ACCi/Feno combinations (Figure S1C). ACCi monotherapy increased blood glucose levels by 30%, and ACCi/Feno combinations normalized blood glucose levels (Figure S1D). ACCi monotherapy increased plasma TG by 29%, and this was completely normalized with ACCi/Feno combinations (Figure 1G). Fasted plasma ApoC3 levels were dose-dependently decreased with Feno monotherapy and ACCi/Feno combinations ($p \leq 0.05$ vs. ACCi) (Figure 1H). Serum total cholesterol levels were significantly lowered by 14%–20% with ACCi monotherapy and ACCi/Feno combinations, versus vehicle (Figure S1E).

We next assessed whether the improvements in liver TG and metabolic homeostasis resulted in improvements in liver health and NASH-related endpoints. Lipid peroxidation, a marker of lipotoxicity-induced oxidative stress, was significantly reduced by 23% and 35% with ACCi monotherapy and ACCi/Feno^{low} combination, respectively (Figure 1I). Liver F4/80$^+$ area, indicative of macrophage infiltration, was significantly reduced with Feno monotherapy and ACCi/Feno combinations versus vehicle (Figure 1J and Figure S1F). Although the mouse FFD model does not develop appreciable fibrosis, hepatic collagen type I alpha 1 chain (*Col1a1*) messenger RNA expression was induced 27-fold in

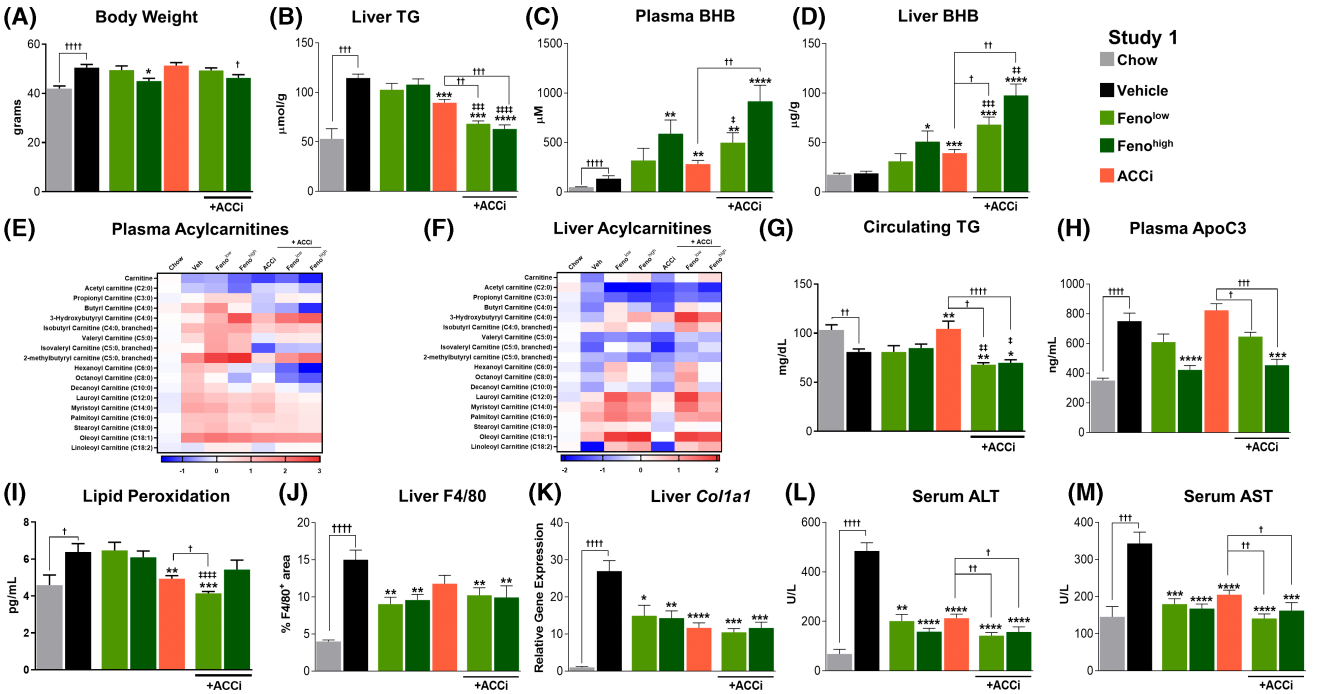

FIGURE 1 Effect of the analogue of firsocostat (ACCi) and fenofibrate (Feno) as monotherapies or in combination in fast-food diet (FFD)–fed mice. Terminal body weight (A), liver triglycerides (TG) (B), plasma β-hydroxybutyrate (BHB) (C), liver BHB (D), plasma acylcarnitine (E), liver acylcarnitine (F), and circulating TG (G) collected in the fed state, 2 h following dose, after 15 days of dosing. (H) Plasma ApoC3 collected after a short fast after 14 days of dosing. (I) Terminal hepatic lipid peroxidation assessed by malondialdehyde content. (J) Quantitation of hepatic F4/80$^+$ immunostaining. (K) Hepatic collagen type I alpha 1 chain (*Col1a1*) expression. (L,M) Serum alanine aminotransferase (ALT) and aspartate aminotransferase (AST) levels. Unless otherwise specified, data are presented as mean ± SEM (n = 10–15 animals/group). In (E) and (F), data are presented as $\log_2$(fold change relative to chow), and in (K) data are presented as fold change relative to chow. *$p \le 0.05$, **$p \le 0.01$, ***$p \le 0.001$, ****$p \le 0.0001$ versus vehicle; $^{\dagger}p \le 0.05$, $^{\dagger\dagger}p \le 0.01$, $^{\dagger\dagger\dagger}p \le 0.001$, $^{\dagger\dagger\dagger\dagger}p \le 0.0001$ versus ACCi monotherapy, or as indicated; $^{\ddagger}p \le 0.05$, $^{\ddagger\ddagger}p \le 0.01$, $^{\ddagger\ddagger\ddagger}p \le 0.001$, $^{\ddagger\ddagger\ddagger\ddagger}p \le 0.0001$ versus Feno^{low} or Feno^{high} monotherapy.

the model and significantly lowered by 44%–61% in all groups (Figure 1K). Serum ALT and AST levels were significantly reduced by 40%–71% with all treatments; ACCi/Feno combinations were more effective than ACCi monotherapy (Figure 1L,M). In summary, ACCi and Feno combination synergistically increased hepatic lipid metabolism and improved several indices of NASH in a mouse model of early NASH.

PPAR agonists exhibit expected potency and selectivity against human PPARs

Given the beneficial effects of ACCi/Feno combination on lowering ACCi-induced plasma TG increase and lowering liver TG, we next evaluated whether combinations of ACCi with other PPAR agonists would also result in similar benefits. We first profiled the potency and PPAR isoform selectivity of the agonists (Ela, Lani, Sela, and Saro) head-to-head against Feno in luciferase reporter assays against human and rodent PPARα, PPARδ, and PPARγ (Table S2). All agents demonstrated the expected PPAR isoform selectivity against human PPARα, PPARδ, and PPARγ. PPAR isoform selectivity was preserved against mouse and rat PPARs for all PPAR agonists tested except Lani, which was a pan-PPAR agonist in the human and mouse assays but did not activate rat PPARδ, as previously reported.[25] Saro equipotently activated PPARα and PPARγ in all species. Feno, Ela, and Sela demonstrated activity against human and rodent PPARγ, although at lower potencies than their primary activity against PPARα or PPARδ (Table S2).

Effect of test agents on hepatocyte FAO *in vitro*

ACCi/Feno combination synergistically increased FAO in the mouse FFD model (Figure 1). Therefore, we developed an *in vitro* assay to evaluate the combination potential of ACCi with other PPAR agonists to augment FAO. The assay was optimized in the Huh7 human hepatocellular carcinoma cell line and primary rat hepatocytes, and measured the incorporation of ^{14}C-labeled oleic acid or palmitic acid into acid soluble lipids (Figure S2A). FIR demonstrated comparable FAO EC_{50} using either tracer in the Huh7 cells (^{14}C-OA = 32.7 nM; ^{14}C-PA = 16.6 nM) and rat hepatocytes

(^{14}C-OA = 18.5 nM; ^{14}C-PA = 8.4 nM) (Figure S2B). The assay was further validated using etomoxir, a carnitine palmitoyl transferase 1 (CPT1) inhibitor, that blocked FAO with an EC_{50} of 136 nM (Figure S2C). Due to larger dynamic range and differences in pharmacology of PPAR agonists in human and rodents,[26–28] ^{14}C-OA tracer was used to assess FAO in Huh7 cells in subsequent experiments.

ACCi induced FAO about 3 times with an EC_{50} of 14.5 nM (Figure 2A). Fenofibric acid, the active form of Feno, was not active in the FAO assay up to a concentration of 100 μM. Ela (α/β) and Saro (α/γ) were less potent than ACCi and activated FAO by 1.4 times, 3.6 times with EC_{50} of 10.3 μM, 51.5 μM, respectively, whereas Sela (β) and Lani (pan) did not stimulate FAO at the concentrations tested (Figure 2A,B). Combining ACCi at about EC_{50} concentration with a dose range of Ela or Saro increased E_{max} by 142% and 120%, respectively, without altering the EC_{50} (Figure 2A,B).

The activity of Res (THRβ agonist) was also assessed in this assay. Similar to Ela and Saro, Res induced FAO by 1.6 times with an EC50 of 46.0 μM. In combination with ACCi, the E_{max} of Res increased 158% without altering the EC_{50} (Figure 2A,B).

ACCi lowers liver TG and increases serum TG in dyslipidemic rat model

ACCi-induced hypertriglyceridemia in the clinic is observed in subjects with elevated baseline TG,[17] and we mimicked this preclinically in a dyslipidemic rat model in which rats were fed FFD for 4 weeks. Unlike the FFD-fed mice, in which plasma TGs are unchanged or lowered relative to chow controls (Figure 1G), FFD-fed rats develop significant and sustained dyslipidemia (3.2 times increase in circulating TG vs. chow) within 1 week of FFD feeding (Figure S3).

The effect of ACCi on liver and circulating TG was evaluated in dyslipidemic rats fed FFD for a total of 4 weeks, and treated with 10 or 30 mg/kg of ACCi, doses that achieve partial (57%–73%) DNL

(A)

Compound Name	Compound MOA	EC50, nM	EC50 (in presence of 20nM ACCi), nM	FAO increase -/+ 20nM ACCi, %
Feno	PPARα agonist	>100,000	>100,000	-
Ela	PPARα/δ agonist	10,334	5172 ± 2012	142
Saro	PPARα/γ agonist	51,569	44.692	120
Sela	PPARδ agonist	>100,000	>100,000	-
Lani	Pan-PPAR agonist	>100,000	>100,000	-
Res	THRβ agonist	43,645	43,501	158

(B)

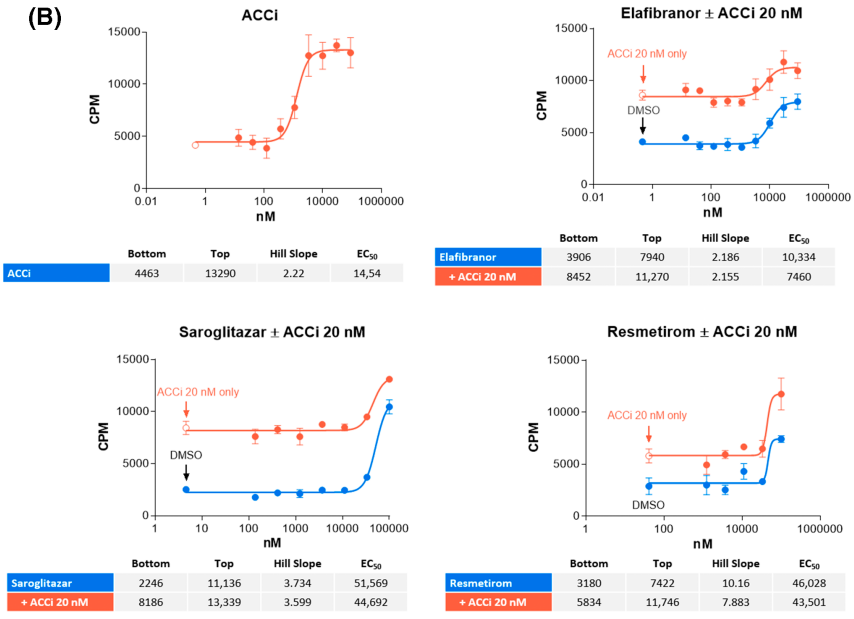

FIGURE 2 Effects of peroxisome proliferator-activated receptor (PPAR) (Feno, elafibranor [Ela], lanifibranor [Lani], seladelpar [Sela], and saroglitazar [Saro]) and thyroid hormone receptor beta (THRβ) (Res) agonists on fatty acid oxidation (FAO) alone or in combination with ACCi. (A) Activity of PPAR (Feno, Ela, Lani, Sela, and Saro) and THRβ (Res) agonists alone or in combination with ACCi on FAO in Huh7 cells. (B) Representative curves for FAO induction in Huh7 cells with ACCi or PPAR/THRβ agonists alone or in combination with ACCi (at ~EC_{50} concentration). Data are presented as mean ± SD.

inhibition in lean rats,[14] from Week 2 to 4. ACCi dose-dependently decreased liver TG by 27%–41% ($p \leq 0.01$ vs. vehicle) and significantly increased fasted circulating TG by 20%–46% (Figure S3A–C), without altering body weight. The effect of ACCi on circulating TG was more consistent in animals dosed with 30 mg/kg than 10 mg/kg (Figure S3C). Across two independent studies, ACCi consistently increased predose, fasted circulating TG relative to baseline (no test article) (Figure S3D). Thus, in subsequent combination studies, ACCi was dosed at 30 mg/kg, and longitudinal changes in predose fasted circulating TG were monitored.

Combinations of ACCi with PPAR agonists or Res mitigated circulating TG increase with some synergistic effects on liver TG reduction

Dyslipidemic rats were fed FFD for a total of 28 days and dosed with PPAR agonists or Res starting on Day 7, and ACCi (either alone or in combination with PPAR/THRβ agonist) starting on Day 14 across three independent studies, as described in the Table S1 (Figure S4A). The staggered dosing in this study was designed to mimic the clinical FIR/Feno combination study in subjects with NASH,[17] and Feno was used as a control in the model. No significant change in body weight was observed with test article treatment (Figure S4B).

Feno, Ela, Lani, Sela, and Saro dose-dependently reduced circulating TG by 31%–48%, 37%–63%, 0%–35%, 0%–75%, and 20%–90% relative to vehicle, respectively, while only 3 mg/kg Res reduced circulating TG (50% vs. vehicle) after 1 week of treatment as a monotherapy (Figure 3A, shaded). All agents also dose-dependently mitigated ACCi-induced circulating TG increase within 1 week of combination dosing (Figure 3A [unshaded] and 3B). Circulating TG were maintained at or below levels in vehicle group when ACCi was dosed in combination with Feno and Ela (at all doses), ≥ 10 mg/kg Lani, ≥ 5 mg/kg Sela, ≥ 0.3 mg/kg Saro, and ≥ 1 mg/kg Res.

Terminal liver TG content was reduced by 41%–69% by 30 mg/kg ACCi monotherapy across three independent studies (Figure 3C). Combining ACCi with Feno, Ela or Res, but not Lani, Sela or Saro, lowered liver TG relative to ACCi alone (Figure 3C). Compared with vehicle, liver TG was reduced by 41% with ACCi alone, and by 58% and 76%, respectively, with 15 mg/kg Feno and 30 mg/kg Ela combinations in Study 2 ($p \leq 0.05$ vs. ACCi alone). Similarly, in Study 4, liver TG was lowered by 69% by ACCi

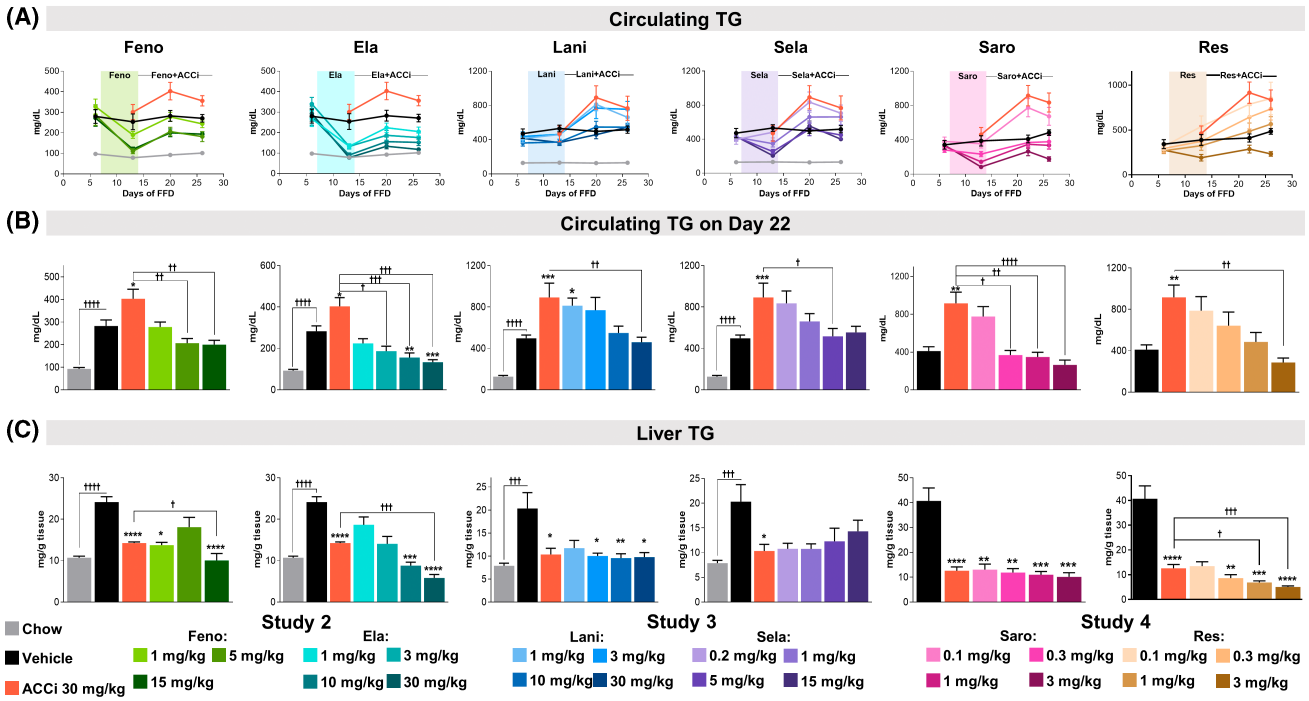

FIGURE 3 Effect of combinations of ACCi with PPAR/THRβ agonists on liver and circulating TG in dyslipidemic rats. (A) Longitudinal circulating TG with PPAR/THRβ agonists treated as monotherapy (shaded area) or in combination with ACCi. (B) Circulating TG on Day 22 of FFD feeding, 2 weeks after initiation of PPAR agonist treatment and 1 week after initiation of ACCi treatment (n = 5–10/group). (C) Terminal liver TG, collected in the fed state, 8 h after dose. Data were generated across three independent studies as described in Table S1, and circulating TG were measured in serum (Study 2) and plasma (Studies 3–4). Data are presented as mean ± SEM (n = 8–10 animals/ group); *$p \leq 0.05$, **$p \leq 0.01$, ***$p \leq 0.001$, ****$p \leq 0.0001$ versus vehicle; $^{\dagger}p \leq 0.05$, $^{\dagger\dagger}p \leq 0.01$, $^{\dagger\dagger\dagger}p \leq 0.001$, $^{\dagger\dagger\dagger\dagger}p \leq 0.0001$ versus ACCi monotherapy, or as indicated.

alone, and by 83% and 88%, respectively, with 1 mg/kg and 3 mg/kg Res combinations ($p \leq 0.05$ vs. ACCi alone).

Terminal plasma and liver exposures of all test articles increased dose-dependently, and Sela, Saro, and Res demonstrated 535-times, 39-times, and 5-times liver loading, respectively, at the highest dose administered (Figure S4C). ACCi exposures were similar in the monotherapy and combination groups (data not shown). Gene expression was measured in the liver and epididymal white adipose tissue (eWAT) to determine target engagement (Figure S5). Hepatic *Apoc3* expression, a component of TG-rich very low-density lipoprotein (VLDL) particles,[29] was significantly reduced in ACCi combinations containing ≥5 mg/kg Feno, ≥3 mg/kg Ela, 15 mg/kg Sela, ≥0.3 mg/kg Saro, and 3 mg/kg Res relative to both vehicle and ACCi alone (Figure S5). Similarly, hepatic expression of PPAR targets such as fatty acid binding protein *3* (*Fapb3*), perilipin 2 (*Plin2*), perilipin 5 (*Plin5)*, pyruvate dehydrogenase kinase 4 (*Pdk4*), carnitine palmitoyltransferase I (*Cpt1*), and carnitine palmitoyltransferase 2 (*Cpt2*) was significantly induced in ACCi combinations containing ≥5 mg/kg Feno, ≥3 mg/kg Ela, 15 mg/kg Sela, and ≥0.3 mg/kg Saro. Res dose-dependently increased the expression of THRβ target genes, Iodothyronine Deiodinase 1 (*Dio1*), Malic Enzyme 1 (*Me1*), Peroxisome proliferator-activated receptor gamma coactivator 1-alpha (*Pgc1a*) and thyroid hormone responsive (*Thrsp*), but not glucose-6-phosphatase catalytic subunit 1 (*G6pc*) and cytochrome P450 family 7 subfamily A member 1(*Cyp7a1)* (Figure S5). ACC inhibition induces sterol regulatory element binding protein 1 (SREBP1) activity via feedback mechanisms,[13] resulting in increased expression of *Srebp1* and its downstream targets patatin-like phospholipase domain-containing 3 (*Pnpla3*) and stearoyl-coenzyme A desaturase 1 (*Scd1*). Expression of *Srebp1*, *Pnpla3*, and *Scd1* was induced to a similar extent in ACCi monotherapy and combinations with all PPAR agonists, except for combination with 15 mg/kg Sela, which decreased the expression of these genes versus monotherapy (Figure S5). PPAR target genes in eWAT were induced by 15 mg/kg Sela and 3 mg/kg of Saro (Figure S5b). Res dose-dependently increased eWAT expression of fatty acid binding protein 4 (*Fabp4*), *Glut4, Scd1, Thsrp*, and *Me1*, suggesting THRβ activation in WAT (Figure S5b).

In summary, while all agents dose-dependently reduced ACCi-mediated increase in circulating TG, only compounds agonizing PPARα (Feno and Ela) and Res further reduced liver TG.

Combination with Feno and Res did not augment the antifibrotic activity of ACCi in CDHFD rat model

We have previously shown that ACCi monotherapy inhibits fibrosis progression in the CDHFD rat model of advanced fibrosis, which may in part be mediated by direct effects of ACCi to suppress transforming growth factor β (TGF-β)–mediated HSC activation.[14] None of the PPAR/THRβ agonists had a similar effect to inhibit HSC activation in the LX-2 human HSC cell line (Table S3). ACCi inhibited TGF-β-induced collagen production with an EC_{50} of 11 nM and CC_{50}, a measure of cellular viability, of >35 μM (Table S3).[14] Most of the PPAR/THRβ agonists tested modestly inhibited collagen production in LX-2 cells with EC_{50} >5 μM. Ela inhibited collagen production with EC_{50} of about 2 μM, and CC_{50} of about 4 μM, suggesting that the reduction in collagen production may be due to decreased cellular viability (Table S3).

Given the beneficial effects of ACCi combination with Feno or Res on both circulating and liver TG, we further evaluated the antifibrotic efficacy of the combinations in the rat CDHFD model. Briefly, rats were fed CDHFD for a total of 12 weeks and treated once daily, orally with ACCi (10 mg/kg), Feno (5 mg/kg), Res^{low} (0.3 mg/kg) or Res^{high} (3 mg/kg), as monotherapies or in combination with ACCi from weeks 6–12. A group of animals were necropsied after 6 weeks of CDHFD feeding (baseline) to establish the extent of fibrosis at time of test article dosing. Hepatic fractional PSR^{+}, alpha–smooth muscle actin (α-SMA^{+}), and clusters of differentiation 68 ($CD68^{+}$) area progressively increased in chow (0.7%, 0.2% and 0.9%, respectively), baseline (2.1%, 0.7% and 7.7%, respectively), and vehicle (6.5%, 2.5% and 10.6%, respectively) groups; test article effect on these parameters was normalized to vehicle and baseline (Figure 4A–D).

Plasma and liver exposures, and hepatic target engagement assessed by gene expression (*Srebp1*, *Scd1*, and *Pnpla3* expression for ACCi, *Apoc3*, *Plin5*, and *Pdk4* expression for Feno and *Me1*, *Pgc1a*, and *Thsrp* expression for Res) were similar between monotherapy and combination groups (Figure S6A,B). ACCi, but not Feno or Res, monotherapy significantly reduced PSR^{+} and α-SMA^{+} area by 53% and 74%, respectively (Figure 4A,B,D). ACCi/Feno, but not ACCi/Res, combination tended to further reduce PSR^{+} area (65%) versus ACCi monotherapy (Figure 4A,D). Compared with vehicle, α-SMA^{+} area was significantly reduced by 89%, 52%, and 78% with ACCi/Feno, ACCi/Res^{low}, and ACCi/Res^{high} combinations, respectively (Figure 4B,D). $CD68^{+}$ area was lowered to baseline levels with ACCi/Feno and ACCi/Res^{high} combinations ($p \leq 0.05$ vs. vehicle, and either monotherapy) (Figure 4C,D).

Changes in plasma biomarkers of liver function and health, including Enhanced Liver Fibrosis components (hyaluronic acid [HA], TIMP1, and procollagen type 3), alpha 2 macrogobulin (A2M) and cytokeratin 18 (CK18)-M30 fragment, were comparable to histological changes (Table 1). ACCi monotherapy significantly lowered plasma HA and A2M, while Res^{high}

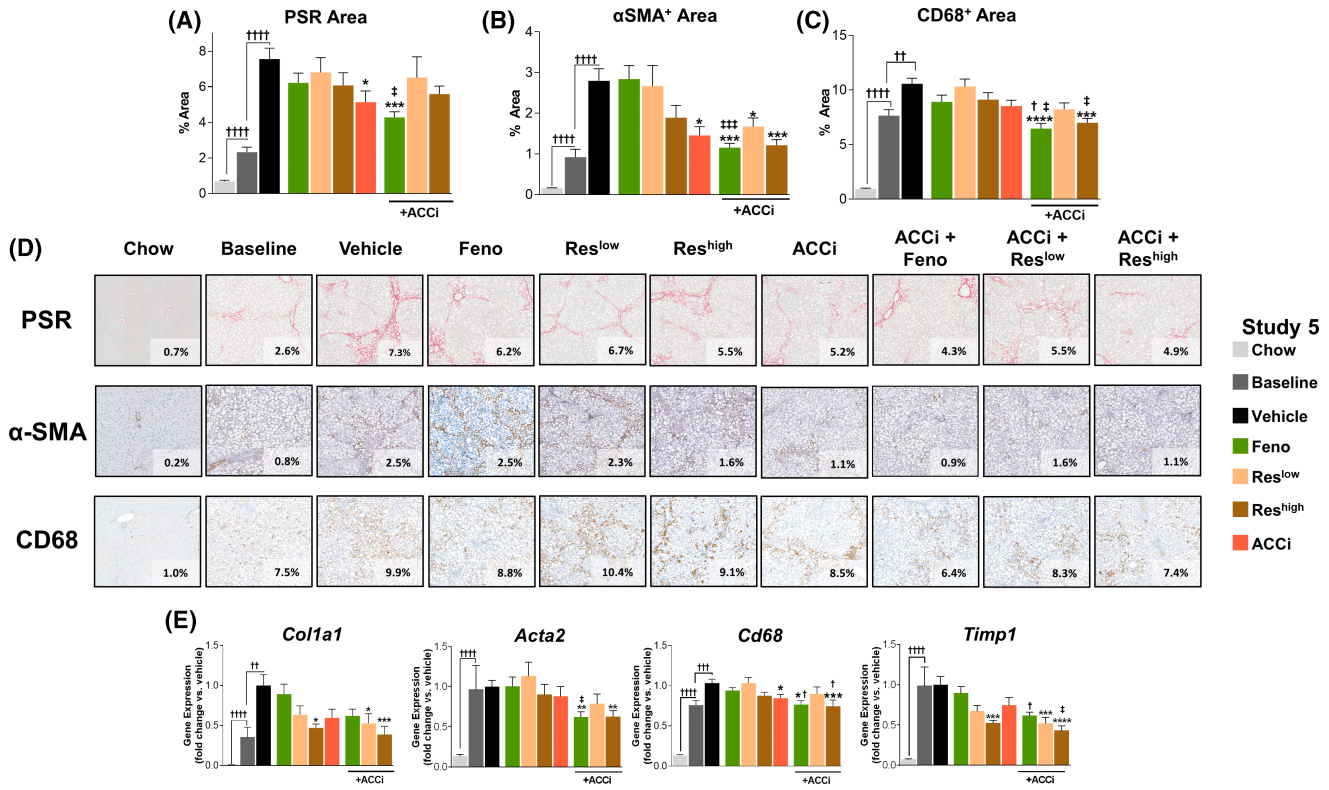

FIGURE 4 Effect of ACCi, Feno, and Res treatment as monotherapies or in combination with ACCi in the choline-deficient high-fat diet (CDHFD) rat model. (A–D) Quantification and representative images of hepatic picrosirius red (PSR) staining, and alpha–smooth muscle actin (α-SMA$^+$), and clusters of differentiation 68 (CD68$^+$) area as assessed by immunohistochemistry. (E) Terminal hepatic expression of fibrosis, fibrogenesis, and immune markers; data are presented as fold change relative to chow. Data are presented as mean ± SEM (n = 10–15 animals/ group); *$p \leq 0.05$, **$p \leq 0.01$, ***$p \leq 0.001$, ****$p \leq 0.0001$ versus vehicle; $^{\dagger}p \leq 0.05$, $^{\dagger\dagger}p \leq 0.01$, $^{\dagger\dagger\dagger}p \leq 0.001$, $^{\dagger\dagger\dagger\dagger}p \leq 0.0001$ versus ACCi monotherapy, or as indicated; $^{\ddagger}p \leq 0.05$, $^{\ddagger\ddagger}p \leq 0.01$, $^{\ddagger\ddagger\ddagger}p \leq 0.001$, $^{\ddagger\ddagger\ddagger\ddagger}p \leq 0.0001$ versus Feno, Res^{low}, or Res^{high} monotherapy. Abbreviation: TIMP1, tissue inhibitor of metalloproteinase 1.

monotherapy significantly lowered plasma TIMP1 and CK18-M30, relative to vehicle. ACCi/Feno combination significantly lowered all biomarkers except CK18-M30, while Res/ACCi combinations dose-dependently reduced all biomarkers. However, none of the combinations significantly reduced biomarkers relative to ACCi monotherapy, with CK18-M30 levels tending to be lower across all combination groups relative to ACCi monotherapy.

Hepatic *Col1a1* expression was dose-dependently reduced by Res (monotherapy and combination), while *Acta2* expression (which encodes α-SMA protein) was decreased only in the ACCi/Feno and ACCi/Res^{high} combination arms (Figure 4E). Reduction in hepatic *Cd68* expression correlated with the trend observed for CD68$^+$ area (Figure 4C), and hepatic *Timp1* expression was dose-dependently reduced only by Res (monotherapy and combination) (Figure 4E). Liver TG in the model inversely correlates with fibrosis progression, and no further reduction was observed with test article treatment (Figure S6C). Liver total cholesterol content was dose-dependently reduced only by Res (monotherapy and combination) (Figure S6D). In sum, combinations of ACCi with Feno or Res did not prevent fibrosis progression beyond ACCi alone in the rat CDHFD model.

DISCUSSION

Hepatic lipotoxicity is hypothesized to play a central role in the pathogenesis of NASH and fibrosis.[7] DNL is up-regulated in subjects with NAFLD/NASH,[8] and targeting this pathway via ACC inhibition simultaneously suppresses DNL and increases FAO, resulting in reduced liver TG accumulation and hepatocyte lipotoxicity.[10] FIR, an allosteric ACC inhibitor, resulted in 30% reduction in relative liver TG in subjects with NASH, and a concomitant increase in plasma TG in subjects with high baseline plasma TG.[11,12] ACCi-induced hypertriglyceridemia, which is also observed preclinically, may be mediated by reduced hepatic PPARα activity, resulting in increased VLDL-TG production and secretion and/or reduced VLDL clearance.[13,16] Here we hypothesized that combining ACCi with PPAR or THRβ agonists could further reduce hepatic lipotoxicity via complementary mechanisms, and therefore augment NASH and antifibrotic efficacy while mitigating

TABLE 1 Effect of test articles on terminal plasma levels of biomarkers of fibrosis in the CDHFD rat model

	Controls			Monotherapy				Combinations		
Parameter	Chow	Start	Vehicle	Feno	Res^{low}	Res^{high}	ACCi	ACCi + Feno	ACCi + Res^{low}	ACCi + Res^{high}
HA	21±2	27±4	59±7[a]	52±4	47±5	43±2	36±4[b]	36±3[b,c]	48±4	36±2[b]
TIMP1	6±1	44±6[a]	47±4[a]	42±3	43±3	29±2[b]	33±3	30±2[b,c]	31±3[b,c]	27±1[b]
PIIINP	7±0.3	24±2[a]	25±1[a]	25±1	28±2	22±1	20±2	19±1[b,c]	23±1	18±1[b]
A2M	20±1	63±10[a]	416±59[a]	296±30	352±47	274±42	207±32[b]	156±19[b,c]	251±45[b]	186±30[b]
CK18-M30	35±4	318±40[a]	358±30[a]	414±32	305±25	221±17[b]	318±34	269±24[c]	235±19[b]	214±13[b]

Note: Data are presented as mean±SEM.

Abbreviations: A2M, alpha 2 macrogobulin; CK18, cytokeratin 18; HA, hemagglutinin; PIIINP, procollagen type 3.

[a] $p<0.05$ versus chow.

[b] $p<0.05$ versus vehicle.

[c] $p<0.05$ versus Feno, Res^{low}, or Res^{high} monotherapy.

ACCi-induced hypertriglyceridemia. Liver TG reduction was used as a primary endpoint to evaluate the combination potential of ACCi with PPAR/THRβ agonists. Although liver TG reduction *per se* is not indicative of NASH efficacy, a growing body of data suggests that greater liver fat reduction is associated with improvements in histological endpoints of NASH resolution and fibrosis regression.[30–32]

PPAR agonists, which have been used extensively in the treatment of dyslipidemia and type 2 diabetes, demonstrate differential effects on NASH resolution and fibrosis regression, which may be due to differences in tissue distribution and/or PPAR isoform selectivity, resulting in varied pharmacology in target tissues.[18] Feno, a specific PPARα agonist, has inconsistent effects on NASH and fibrosis in the clinic.[18] Similarly, Ela, a PPARα/δ dual agonist with about 200-times greater potency than Feno, was not efficacious in a Phase 3 trial.[18] Lani, a pan-PPAR agonist with preferential PPARγ agonism, demonstrated both fibrosis regression (42% vs. 24% placebo) and NASH resolution (45% vs. 19% placebo) over 24 weeks, and is being evaluated in a Phase 3 trial for NASH.[33] Similarly, while not evaluated in this study, another PPARγ agonist pioglitazone, previously been approved for type 2 diabetes, also improved NASH resolution (47% vs. 21% placebo) without any effects on fibrosis progression.[34] Sela, a selective PPARδ agonist, improved NASH resolution (26% vs. 8% placebo) over 52 weeks, although the trial was terminated due to unexpected histological findings, later deemed to be not test article–related.[35] Saro, a PPARα/γ dual agonist, reduced liver fat over 16 weeks in subjects with NAFLD.[36]

THRβ agonists represent another class of dyslipidemic agents that induce transcription of genes involved in fatty acid and cholesterol uptake and metabolism, thereby reducing hepatocyte lipotoxicity and promoting NASH resolution.[33,37] Liver-directed THRβ agonists, currently in clinical development for NASH, afford a strategy to safely target the THR signaling axis and have demonstrated NASH resolution in clinical trials with significant liver TG reduction and plasma lipid improvements.[33] Res, the most advanced THRβ agonist currently in a Phase 3 NASH trial, demonstrated NASH resolution (27.4% vs. 6.5% placebo) in subjects with NASH.[19]

ACCi, Ela, Saro, and Res increased FAO *in vitro* as monotherapies, in line with expected biology. However, while ACCi was very potent (EC_{50} = 8–33 nM) at inducing FAO, the other agents were not (Figure 2). This could reflect different mechanisms for FAO induction for these agents. ACC inhibition releases the post-translational inhibition of CPT1, a rate-limiting enzyme in FAO, by malonyl CoA, whereas PPAR/THRβ agonism up-regulates transcription of FAO genes. Indeed, under certain conditions, including THRβ overexpression or longer duration of treatment, FAO induction and/

or reduction in cellular lipid accumulation have been reported with PPAR/THRβ agonists.[38,39] Although the combination of ACCi with Ela, Saro, and Res increased E_{max}, there was no effect on EC_{50}, suggesting some synergism on FAO activation, which was also observed in liver TG reduction in the dyslipidemic rat model.

ACCi combination with Feno or Ela, but not Lani, Sela or Saro, dose-dependently augmented liver TG reduction in the dyslipidemic rat model, suggesting that PPARα agonism (afforded by Feno and Ela) drives liver TG reduction (Figure 3). This may be driven by a synergistic increase in hepatic FAO, as demonstrated by increased plasma BHB and decreased acylcarnitine levels with ACCi + Feno combination in the FFD mouse (Figure 1). The differential effect of the PPAR agonists on liver TG could reflect distinct pharmacology due to PPAR isoform selectivity of these agents,[18] or differential rodent versus human PPAR isoform selectivity/potency of agents such as that observed with Lani (Table S2). Saro, an equipotent dual PPARα/γ agonist, did not further reduce liver TG in combination with ACCi, despite inducing a similar FAO gene signature to Feno and Ela (Figure S5). This may be due to PPARγ-induced hepatic steatosis, reported in mice with hepatic-specific PPARγ overexpression,[40] which may offset PPARα-driven increases in FAO. Similarly, Sela, a potent and selective PPARδ agonist, also did not augment ACCi-induced liver TG reduction which is in line with reports of PPARδ overexpression and/or agonism inducing the expression of DNL genes and inconsistent effects of PPARδ agonists on hepatic steatosis.[40] Dose-dependent effects of Feno and Ela to augment ACCi-induced liver TG reduction in rodents is contrary to their reported effects in humans and may reflect rodent-specific pharmacology of PPAR agonism to increase peroxisomal proliferation and FAO[27] and/or supra-pharmacological doses. Dose-dependent induction of peroxisomal markers were observed in the livers of rodents treated with PPAR agonists in this study (data not shown). Clinical FIR combination with 48 and 145 mg of Feno in subjects with NASH did not augment liver TG reduction over 24 weeks, although interpretation of the data is confounded by the lack of a FIR monotherapy group.[17] Therefore, the translation of these preclinical findings to clinical liver TG reduction in the setting of combinations is still unclear.

Res dose-dependently reduced liver TG in combination with ACCi and induced a different hepatic gene signature to PPAR agonists (Figure S5). Interestingly, while Res demonstrated some liver loading (4–5 times), THRβ target genes (*Me1* and *Thsrp*) were also dose-dependently induced in the adipose tissue (Figures S4 and S5), suggesting THRβ agonism in that tissue. Thyroid hormone signaling induces genes involved in carbohydrate and lipid metabolism, and thermogenesis in the adipose tissue.[41] It is unclear whether Res exposures achieved in this study are clinically relevant, nor has THRβ target engagement in adipose tissue previously been reported with Res.

All PPAR/THRβ agonists tested dose-dependently reduced circulating TG as monotherapies and mitigated ACCi-induced hypertriglyceridemia (Figure 3). The effect of PPAR agonists on circulating TG levels are mediated by decreased ApoC3 production, resulting in reduced hepatic VLDL-TG secretion and increased plasma LPL activity and conserved between rodents and humans.[13,16] Indeed, co-dosing FIR with Feno completely mitigated FIR-induced plasma TG increase in subjects with NASH.[17] Furthermore, PPAR agonists affected circulating TG at lower doses than needed for liver TG reduction in dyslipidemic rats (Figure 3). In contrast, the efficacious doses of Res to lower circulating TG was similar to doses needed for liver TG reduction. This may reflect different mechanisms by which Res affects hepatic lipid metabolism, including the induction of autophagy.[42]

ACC inhibition directly inhibits HSC activation *in vitro*, which may also contribute to its antifibrotic efficacy *in vivo*.[14] ACCi combination with Feno or Res did not significantly augment antifibrotic efficacy in CDHFD-fed rats, although PSR reduction with ACCi + Feno combination tended to be greater than ACCi alone. This is in line with observations of dose-dependent reductions in liver stiffness (27%–32%) in subjects with NASH co-dosed with FIR and 48 or 145 mg of Feno.[17] Neither Feno nor Res monotherapy inhibited fibrosis progression. The dose of Feno in this study was targeted to match exposures of the clinical 145-mg Feno dose; therefore, the lack of an antifibrotic effect is not surprising. Furthermore, Res monotherapy did not promote fibrosis regression in subjects with NASH; however exposure-related effects were observed on histological NASH resolution.[43] The 3-mg/kg Res dose achieved approximately 2-fold lower terminal hepatic concentrations in the CDHFD rats than the dyslipidemic rats (Figures S4 and S6). Although THRβ target engagement was observed, it is also possible that the exposures achieved in the CDHFD rats were below clinically efficacious exposures. Our data are also in line with a recent report of Res improving NAFLD activity score but not fibrosis score in a DIO-NASH mouse model.[24] Res monotherapy also tended to reduce α-SMA$^+$ and CD68$^+$ area in the CDHFD rat model, which is in line with reported observations in the DIO-NASH mouse model.[24] PPARγ expression has been associated with HSC quiescence, and indeed treatment of rodent or human HSCs with ACCi also increased PPARγ expression while concomitantly reducing HSC activation.[14] In addition, Lani and pioglitazone, predominantly PPARγ agonists, demonstrate beneficial effects on NASH resolution and fibrosis regression in human subjects.[33,34] Although Lani did not demonstrate potent, direct antifibrotic activity in the LX-2

cells, it is possible that combination of ACCi with Lani may have additive effects to reduce fibrosis progression *in vivo*, which was not evaluated in this study.

Taken together, this study identifies the potential benefit of combining PPAR or THRβ agonists with an ACCi to augment liver and/or circulating TG reduction relative to ACCi monotherapy. However, this combination strategy may not provide greater antifibrotic efficacy, suggesting that strategies targeting hepatocyte lipid metabolism alone may not be sufficient to improve fibrosis regression in subjects with NASH.

CONFLICT OF INTEREST

D.B., M.T., J.T., D.H., B.M., A.V., J.B., and J.T. own stock in Gilead.

REFERENCES

1. Williams CD, Stengel J, Asike MI, Torres DM, Shaw J, Contreras M, et al. Prevalence of nonalcoholic fatty liver disease and nonalcoholic steatohepatitis among a largely middle-aged population utilizing ultrasound and liver biopsy: a prospective study. Gastroenterology. 2011;140:124–31.
2. Ong JP, Younossi ZM. Epidemiology and natural history of NAFLD and NASH. Clin Liver Dis. 2007;11:1–16, vii.
3. Younossi ZM, Koenig AB, Abdelatif D, Fazel Y, Henry L, Wymer M. Global epidemiology of nonalcoholic fatty liver disease—meta-analytic assessment of prevalence, incidence, and outcomes. Hepatology. 2016;64:73–84.
4. Vernon G, Baranova A, Younossi ZM. Systematic review: the epidemiology and natural history of non-alcoholic fatty liver disease and non-alcoholic steatohepatitis in adults. Aliment Pharmacol Ther. 2011;34:274–85.
5. Afzali A, Berry K, Ioannou GN. Excellent posttransplant survival for patients with nonalcoholic steatohepatitis in the United States. Liver Transpl. 2012;18:29–37.
6. Wong RJ, Aguilar M, Cheung R, Perumpail RB, Harrison SA, Younossi ZM, et al. Nonalcoholic steatohepatitis is the second leading etiology of liver disease among adults awaiting liver transplantation in the United States. Gastroenterology. 2015;148:547–55.
7. Neuschwander-Tetri BA. Hepatic lipotoxicity and the pathogenesis of nonalcoholic steatohepatitis: the central role of nontriglyceride fatty acid metabolites. Hepatology. 2010;52:774–88.
8. Donnelly KL, Smith CI, Schwarzenberg SJ, Jessurun J, Boldt MD, Parks EJ. Sources of fatty acids stored in liver and secreted via lipoproteins in patients with nonalcoholic fatty liver disease. J Clin Invest. 2005;115:1343–51.
9. Vuppalanchi R, Noureddin M, Alkhouri N, Sanyal AJ. Therapeutic pipeline in nonalcoholic steatohepatitis. Nat Rev Gastroenterol Hepatol. 2021;18:373–92.
10. McGarry JD, Mannaerts GP, Foster DW. A possible role for malonyl-CoA in the regulation of hepatic fatty acid oxidation and ketogenesis. J Clin Invest. 1977;60:265–70.
11. Loomba R, Kayali Z, Noureddin M, Ruane P, Lawitz EJ, Bennett M, et al. GS-0976 reduces hepatic steatosis and fibrosis markers in patients with nonalcoholic fatty liver disease. Gastroenterology. 2018;155:1463–73.e1466.
12. Lawitz EJ, Coste A, Poordad F, Alkhouri N, Loo N, McColgan BJ, et al. Acetyl-coa carboxylase inhibitor gs-0976 for 12 weeks reduces hepatic de novo lipogenesis and steatosis in patients with nonalcoholic steatohepatitis. Clin Gastroenterol Hepatol. 2018;16:1983–91.e1983.
13. Goedeke L, Bates J, Vatner DF, Perry RJ, Wang T, Ramirez R, et al. Acetyl-CoA carboxylase inhibition reverses NAFLD and hepatic insulin resistance but promotes hypertriglyceridemia in rodents. Hepatology. 2018;68:2197–211.
14. Bates J, Vijayakumar A, Ghoshal S, Marchand B, Yi S, Kornyeyev D, et al. Acetyl-CoA carboxylase inhibition disrupts metabolic reprogramming during hepatic stellate cell activation. J Hepatol. 2020;73:896–905.
15. Bergman A, Carvajal-Gonzalez S, Tarabar S, Saxena AR, Esler WP, Amin NB. Safety, tolerability, pharmacokinetics, and pharmacodynamics of a liver-targeting acetyl-CoA carboxylase inhibitor (PF-05221304): a three-part randomized phase 1 study. Clin Pharmacol Drug Dev. 2020;9:514–26.
16. Kim CW, Addy C, Kusunoki J, Anderson NN, Deja S, Fu X, et al. Acetyl CoA carboxylase inhibition reduces hepatic steatosis but elevates plasma triglycerides in mice and humans: a bedside to bench investigation. Cell Metab. 2017;26:394–406.e396.
17. Lawitz EJ, Neff G, Ruane PJ, Younes Z, Zhang J, Jia C, et al. Fenofibrate mitigates increases in serum triglycerides due to the ACC inhibitor firsocostat in patients with advanced fibrosis due to NASH: a phase 2 randomized trial. Hepatology. 2019;70:1489A–90A.
18. Cariello M, Piccinin E, Moschetta A. Transcriptional regulation of metabolic pathways via lipid-sensing nuclear receptors PPARs, FXR, and LXR in NASH. Cell Mol Gastroenterol Hepatol. 2021;11:1519–39.
19. Alkhouri N. Thyromimetics as emerging therapeutic agents for nonalcoholic steatohepatitis: rationale for the development of resmetirom (MGL-3196). Expert Opin Investig Drugs. 2020;29:99–101.
20. Wettstein G, Luccarini JM, Poekes L, Faye P, Kupkowski F, Adarbes V, et al. The new-generation pan-peroxisome proliferator-activated receptor agonist IVA337 protects the liver from metabolic disorders and fibrosis. Hepatol Commun. 2017;1:524–37.
21. Haczeyni F, Wang H, Barn V, Mridha AR, Yeh MM, Haigh WG, et al. The selective peroxisome proliferator-activated receptor-delta agonist seladelpar reverses nonalcoholic steatohepatitis pathology by abrogating lipotoxicity in diabetic obese mice. Hepatol Commun. 2017;1:663–74.
22. Jain MR, Giri SR, Trivedi C, Bhoi B, Rath A, Vanage G, et al. Saroglitazar, a novel PPARalpha/gamma agonist with predominant PPARalpha activity, shows lipid-lowering and insulin-sensitizing effects in preclinical models. Pharmacol Res Perspect. 2015;3:e00136.
23. Tolbol KS, Kristiansen MN, Hansen HH, Veidal SS, Rigbolt KT, Gillum MP, et al. Metabolic and hepatic effects of liraglutide, obeticholic acid and elafibranor in diet-induced obese mouse models of biopsy-confirmed nonalcoholic steatohepatitis. World J Gastroenterol. 2018;24:179–94.
24. Kannt A, Wohlfart P, Madsen AN, Veidal SS, Feigh M, Schmoll D. Activation of thyroid hormone receptor-beta improved disease activity and metabolism independent of body weight in a mouse model of non-alcoholic steatohepatitis and fibrosis. Br J Pharmacol. 2021;178:2412–23.
25. Boubia B, Poupardin O, Barth M, Binet J, Peralba P, Mounier L, et al. design, synthesis, and evaluation of a novel series of indole sulfonamide peroxisome proliferator activated receptor (ppar) alpha/gamma/delta triple activators: discovery of lanifibranor, a new antifibrotic clinical candidate. J Med Chem. 2018;61:2246–65.
26. Klaunig JE, Babich MA, Baetcke KP, Cook JC, Corton JC, David RM, et al. PPARalpha agonist-induced rodent tumors: modes of action and human relevance. Crit Rev Toxicol. 2003;33:655–780.
27. Lawrence JW, Li Y, Chen S, DeLuca JG, Berger JP, Umbenhauer DR, et al. Differential gene regulation in human versus rodent hepatocytes by peroxisome proliferator-activated receptor (PPAR) alpha. PPAR alpha fails to induce

peroxisome proliferation-associated genes in human cells independently of the level of receptor expresson. J Biol Chem. 2001;276:31521–7.
28. Bility MT, Thompson JT, McKee RH, David RM, Butala JH, Vanden Heuvel JP, et al. Activation of mouse and human peroxisome proliferator-activated receptors (PPARs) by phthalate monoesters. Toxicol Sci. 2004;82:170–82.
29. Boren J, Packard CJ, Taskinen MR. The roles of ApoC-III on the metabolism of triglyceride-rich lipoproteins in humans. Front Endocrinol (Lausanne). 2020;11:474.
30. Loomba R, Guy C, Bedossa P, Taub R, Bashir M, Harrison S. Magnetic resonance imaging-proton density fat fraction (MRI-PDFF) to predict treatment response on NASH liver biopsy: a secondary analysis of the resmetirom randomized placebo-controlled phase 2 clinical trial. J Hepatol. 2020;73:S56.
31. Patel J, Bettencourt R, Cui J, Salotti J, Hooker J, Bhatt A, et al. Association of noninvasive quantitative decline in liver fat content on MRI with histologic response in nonalcoholic steatohepatitis. Therap Adv Gastroenterol. 2016;9:692–701.
32. Stine JG, Munaganuru N, Barnard A, Wang JL, Kaulback K, Argo CK, et al. Change in MRI-PDFF and histologic response in patients with nonalcoholic steatohepatitis: a systematic review and meta-analysis. Clin Gastroenterol Hepatol. 2021;19:2274–83.e2275.
33. Sven MF, Pierre B, Manal FA, Quentin MA, Elisabetta B, Vlad R, et al. A randomised, double-blind, placebo-controlled, multicentre, dose-range, proof-of-concept, 24-week treatment study of lanifibranor in adult subjects with non-alcoholic steatohepatitis: Design of the NATIVE study. Contemp Clin Trials. 2020;98:106170.
34. Sanyal AJ, Chalasani N, Kowdley KV, McCullough A, Diehl AM, Bass NM, et al. NASH CRN. Pioglitazone, vitamin E, or placebo for nonalcoholic steatohepatitis. N Engl J Med. 2010;362:1675–85.
35. Harrison SA, Gunn NT, Khazanchi A, Guy CD, Brunt EM, Moussa S, et al. A 52-week multi-center double-blind randomized phase 2 study of seladelpar, a potent and selective peroxisome proliferator-activated receptor delta (PPAR-DELTA) agonist, in patients with nonalcoholic steatohepatitis (NASH). The Liver Meeting Digital Experience 2020. The Liver Meeting: AASLD; 2020.
36. Goyal O, Nohria S, Goyal P, Kaur J, Sharma S, Sood A, et al. Saroglitazar in patients with non-alcoholic fatty liver disease and diabetic dyslipidemia: a prospective, observational, real world study. Sci Rep. 2020;10:21117.
37. Sinha RA, Singh BK, Yen PM. Direct effects of thyroid hormones on hepatic lipid metabolism. Nat Rev Endocrinol. 2018;14:259–69.
38. Rogue A, Antherieu S, Vluggens A, Umbdenstock T, Claude N, de la Moureyre-Spire C, et al. PPAR agonists reduce steatosis in oleic acid-overloaded HepaRG cells. Toxicol Appl Pharmacol. 2014;276:73–81.
39. Sinha RA, Singh BK, Zhou J, Wu Y, Farah BL, Ohba K, et al. Thyroid hormone induction of mitochondrial activity is coupled to mitophagy via ROS-AMPK-ULK1 signaling. Autophagy. 2015;11:1341–57.
40. Wang Y, Nakajima T, Gonzalez FJ, Tanaka N. PPARs as metabolic regulators in the liver: lessons from liver-specific PPAR-null mice. Int J Mol Sci. 2020;21:2061.
41. Obregon MJ. Adipose tissues and thyroid hormones. Front Physiol. 2014;5:479.
42. Sinha RA, Yen PM. Thyroid hormone-mediated autophagy and mitochondrial turnover in NAFLD. Cell Biosci. 2016;6:46.
43. Harrison SA, Bashir MR, Guy CD, Zhou R, Moylan CA, Frias JP, et al. Resmetirom (MGL-3196) for the treatment of non-alcoholic steatohepatitis: a multicentre, randomised, double-blind, placebo-controlled, phase 2 trial. Lancet. 2019;394:2012–24.

SUPPORTING INFORMATION

Additional supporting information can be found online in the Supporting Information section at the end of this article.

How to cite this article: Vijayakumar A, Okesli-Armlovich A, Wang T, Olson I, Seung M, Kusam S, Combinations of an acetyl CoA carboxylase inhibitor with hepatic lipid modulating agents do not augment antifibrotic efficacy in preclinical models of NASH and fibrosis. Hepatol Commun. 2022;6:2298–2309. https://doi.org/10.1002/hep4.2011